JOURNAL OF GUIDANCE, CONTROL, AND DYNAMICS
Vol. 30, No. 2, March–April 2007

Aircraft Load Alleviation During Maneuvers Using Optimal Control Surface Combinations

Sebastian L. Gaulocher* and Clément Roos†
SUPAERO, F-31055 Toulouse cedex 4, France
and
Christelle Cumer‡
ONERA, F-31055 Toulouse cedex 4, France

DOI: 10.2514/1.25577

Control laws in aeronautics are designed to ensure, above all, good handling qualities. However, during extreme maneuvers, which have to be taken into account for aircraft certification, a number of critical structural load limits cannot be guaranteed by this baseline controller. To avoid some modifications of the control law, a solution consists of judiciously exploiting the redundancy of the control surfaces. The aim of this paper is first to find an optimal strategy of the control surface use, which leaves the initial flight behavior unmodified but alleviates a structural load during a selected maneuver. Model predictive control theory solves this offline control allocation problem under actuator saturation constraints. In addition, an identification procedure is proposed to synthesize a new mixing unit that can reproduce this optimal strategy. This methodology is applied to a flexible transport aircraft to alleviate the bending moment at the external wing during a sudden and strong roll maneuver.

Nomenclature

G	=	vector containing a truncated sequence of the discrete signal g; its elements are typically $g^{(k)}$
$\mathbf{G}$	=	frequency-domain function or frequency response of G
$g^{(k)}$	=	value of the signal g at the sampling time $t_0 + kT_s$; in part III: t_0 is varying; it represents the moment at which the optimization is performed; in part IV: t_0 is equal to 0
M_x	=	bending moment about the x axis at the external wing (between the outer engine and the wing tip)
n_y, n_z	=	lateral and longitudinal load factors
p, r, q	=	roll, yaw, and pitch rates
SPkR	=	right-wing spoiler no. k
SPkL	=	left-wing spoiler no. k
T_s	=	sampling interval
z_{CG}	=	altitude of the center of gravity
α	=	angle of attack
β	=	sideslip angle
ϕ	=	bank angle

I. Introduction

AIRWORTHINESS qualifications require the proof that critical structural loads do not exceed certain limits. This requirement clearly influences the design phase of an aircraft (A/C) and has an impact on later performances. As an example, an A/C has to be capable of compensating the yaw moment induced by an engine loss, hence yielding an oversized rudder. The bottlenecks in A/C design are the requirements, which deal with highly improbable scenarios, for example, the aforementioned engine or a control surface failure. Although these regulations are indispensable for passenger and payload safety, they decisively constrain the controller synthesis phase.

A straightforward way of dealing with this problem is to conceive a standard controller using classical methods (e.g., H_2, H_∞, linear quadratic, linear quadratic Gaussian). This baseline controller fulfills all stability, performance, and robustness criteria. For each scenario of the aforementioned type, an adjusted controller is synthesized. Thus, it becomes possible to treat one problem at a time, while being able to keep the baseline controller during nominal flight. In the *controller tuning* (or *control law adjustment*) phase, the structure of the original controller remains the same, and only some parameters are allowed to change. In aeronautical applications, the gain of a physical meaning associated to these parameters is of prime importance. Figure 1 shows the closed-loop A/C with its nominal controller and the associated mixing unit, whose function is to convert the pitch, roll, and yaw commands into appropriate control effector inputs.

The aim of this paper is to synthesize a new mixing unit without affecting the nominal controller, to limit the amplitudes of certain structural load outputs to an admissible interval while keeping the flight behavior as close as possible to the initial one. Additional amplitude and slew rate constraints applying to the control effector suite also have to be respected.

The first step is to find the best sequence of control effector inputs, which can be formulated as an offline control allocation problem under constraints. The literature is rich with methods suitable for finding the best constrained control vector which ensures a desired achievable control objective via a control effectiveness matrix. According to the norm used for the expression of the optimization criterion, very efficient numerical quadratic programming (pseudoinverse methods [1,2], fixed-point iteration method [3]) or linear programming [4,5] algorithms have been investigated and have given some excellent results. In [6] the solution is obtained by resorting to semidefinite programming. The two requirements, objective realization and effector limits, can be expressed in the form of linear matrix inequalities (LMIs). However the major disadvantage is the difficulty—from a computational point of view—to solve LMIs for large-scale systems. In addition, there is some interesting research at the Virginia Polytechnic Institute [2,7], which is mainly based on a geometrical approach to the control allocation problem. All these methods successfully take into account both amplitude and slew rate saturations of the control effectors. However, there seems to be a lack of methods dealing with output

Received 23 June 2006; accepted for publication 3 October 2006. Copyright © 2006 by ONERA. Published by the American Institute of Aeronautics and Astronautics, Inc., with permission. Copies of this paper may be made for personal or internal use, on condition that the copier pay the $10.00 per-copy fee to the Copyright Clearance Center, Inc., 222 Rosewood Drive, Danvers, MA 01923; include the code 0731-5090/07 $10.00 in correspondence with the CCC.

*Ph.D. Student, Student Member AIAA.
†Ph.D. Student.
‡Research Engineer, System Control and Flight Dynamics Department, 2 avenue Édouard Belin; christelle.cumer@onera.fr.

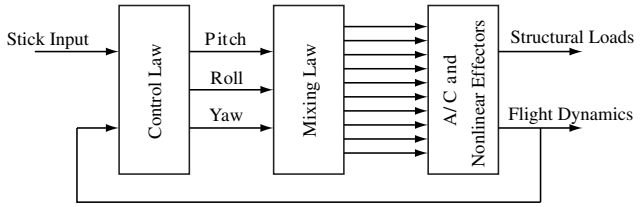

Fig. 1 Closed-loop A/C with the nominal controller and the mixing unit.

constraints. In [8,9], a cascade control method is proposed to respect output constraints, but on the other hand, this method does not offer any possibility to treat control effector saturations. In addition, cascade control has a very particular feedback structure which is not applicable to our case.

In this paper, we thus propose to solve our problem using the model predictive control (MPC) theory. In fact, it is basically a method belonging to the vast area of optimal control methods, proven to be a powerful control method in industrial applications when future reference inputs are known [10–13]. More precisely, a dynamic discrete-time representation of the plant is used to propagate the state in the future. The estimated future state is then exploited to determine control action. The computation of this optimal sequence is usually referred to as the *analysis* phase, since no controller *synthesis* is performed at this stage.

The second step then consists of synthesizing a new mixing law that is able to reproduce this optimal sequence. The idea is to identify the mixing unit in the frequency domain (see [14,15] and references therein). More precisely, efficient methods exist that allow one to identify a fixed-order continuous-time transfer function from time-domain data by minimizing a nonlinear criterion [16,17].

This paper is organized as follows. Section II introduces the industrial application and details the function of the three blocks highlighted in Fig. 1. A reference simulation using the original mixing unit yields the flight behavior to be respected and the load output to be alleviated during the considered scenario, namely, a sudden and strong roll maneuver. Section III then addresses the control allocation problem and presents the model predictive control theory. In Sec. IV, some extensions to this method are highlighted and implemented in the context of the aforementioned maneuver. Section V finally details the identification process that leads to the new mixing unit and presents a few results, which demonstrate the efficiency of the design scheme.

II. Description of the Industrial Application

A. A/C Model and Nonlinear Effectors

The considered application is a flexible transport A/C. The complete linear A/C aeroelastic model (see Fig. 2) has 77 states. Each input corresponds to one control effector: the right and left ailerons (ARW and ALW), the right and left elevators (RE and LE), the rudder (RR), and the *N* right and *N* left spoilers (SP1R to SP*N*R and SP1L to SP*N*L). The outputs can be split into two parts as follows:

1) nine flight dynamics outputs: namely, the sideslip angle, the roll rate, the yaw rate, the bank angle, the lateral load factor, the angle of attack, the pitch rate, the longitudinal load factor, and the altitude of center of gravity;

2) and one structural load output: the bending moment at the external wing about the x axis.

The saturation nonlinearities are upstream with respect to the control effectors. Figure 3 shows the two types of saturations (amplitude and rate saturations) in a signal flow graph.

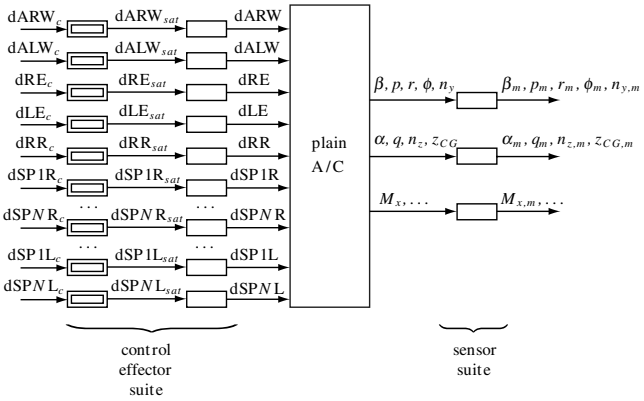

Fig. 2 Fully equipped A/C.

B. Reference Control Law

The nominal controller delivered together with the A/C model uses a part of the aforementioned flight dynamics outputs: n_y, p, r, ϕ, n_z, and q. In addition, the controller receives the pilot's stick and pedal positions as inputs. These positions correspond to the desired roll rate p_{des}, pitch rate q_{des}, and yaw rate r_{des}. The outputs calculated by the controller are the roll rate dp, pitch rate dq, and yaw rate dr to be realized. Figure 4 shows the inputs and outputs of the A/C controller. It is important to note that the longitudinal and lateral parts of the A/C controller are completely separated. However, the roll and yaw movements being coupled, they have to be considered together. Moreover, as the nonlinear A/C model has been linearized about different points concerning Mach number Ma and true air speed v_{TAS}, different controllers have been synthesized for different values of Ma and v_{TAS}.

C. Mixing Law

The commands determined by the control law need to be realized by the control effectors. For this purpose, a mixing technique is applied which has become known under the name of ganging. Linear relationships are used between the controller outputs and the actuator inputs. For the longitudinal flight dynamics, the case is straightforward. As it is decoupled from the lateral flight dynamics, the pitch command dq is made by passing it directly to the pair of elevators via a unity gain (both elevators are deflected by the same angle). Concerning the lateral part of the A/C, the case is slightly different. The ailerons have to be deflected antisymmetrically to yield a roll movement, that is, the right aileron receives dp and the left aileron $-dp$ as input. The value imposed on the rudder is simply dr. It is finally assumed that the spoilers are not used in the considered scenario, therefore the gain connecting the roll channel and the spoilers is zero. Figure 5 illustrates the way the mixing unit of the controller works.

D. Extreme Maneuver

The reference scenario used in the present case is a sudden and strong roll maneuver. Figure 6 shows the temporal shape of this maneuver.

E. Reference Simulation

A reference simulation is performed using the original mixing unit of the A/C controller represented on Fig. 5. The solid lines in Figs. 9 and 14 show the control effector inputs and the flight dynamics and structural load outputs, respectively. The simulation is only run in the interval [0; 10 s], which is sufficient to give an overview of all important occurring phenomena.

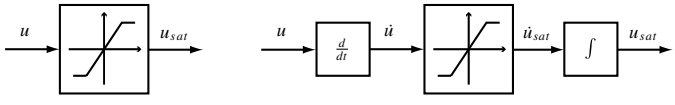

Fig. 3 Amplitude and rate saturations.

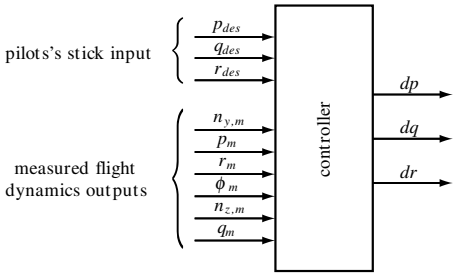

Fig. 4 Inputs and outputs of the A/C controller.

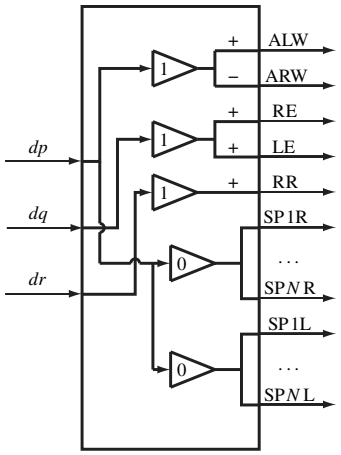

Fig. 5 Mixing unit of the A/C controller.

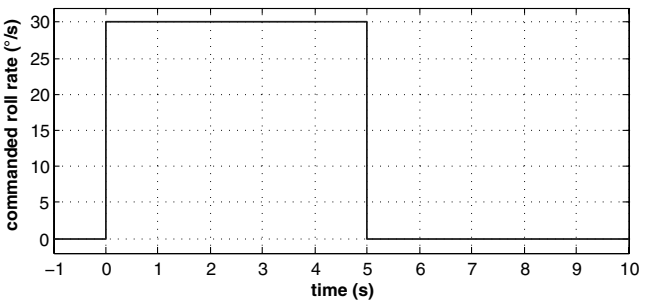

Fig. 6 Reference maneuver.

The amplitude of the left aileron (ALW) is saturated from 0.5 to 1.2 s, and both ailerons are rate saturated from 0.0 to 0.5 s and from 5.0 to 5.6 s, which yields the characteristic ramp behavior. Concerning the structural load output to be alleviated, namely, the bending moment M_x at the external wing, Fig. 14 shows the desired upper and lower bounds at 500,000 and $-500,000$ Nm, respectively. It is important to note that the lower limit is exceeded from 0.5 to 1.5 s, while the upper limit is from 5.7 to 6.2 s.

III. Model Predictive Control Allocation

A. Principle of Model Predictive Control

Figure 7 shows the basic principle of MPC. The important signals are grouped into the input vector u, the tracking output vector y_t, and the constrained output vector y_c. For simplicity, Fig. 7 considers these quantities to be scalars. The horizontal lines "upper bound" and "lower bound" indicate the upper and lower limits, respectively, of the admissible area for the constrained outputs.

A state-space representation of the discretized A/C model is used to predict the various outputs, that is, the tracking outputs (in this case the flight dynamics outputs) and the constrained output (the structural load output). This prediction is performed based on the sequence of control effector inputs U which is yet unknown. Based

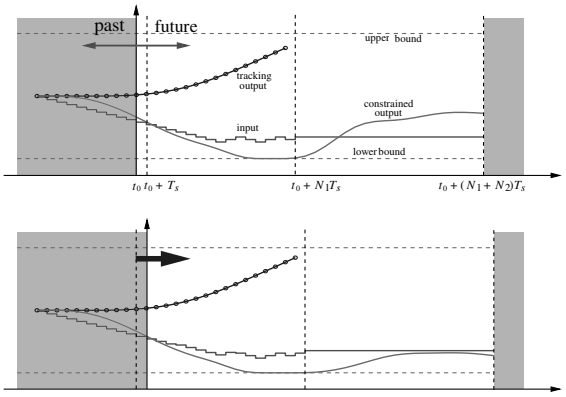

Fig. 7 Principle of model predictive control.

on this prediction, an optimization criterion subject to inequality constraints is formulated. The optimal solution to the criterion, fulfilling the constraints, is the sequence of input vectors $\hat{U}$.

Note that this prediction can only be done over a finite horizon. For the actual point of time t_0, this limit is indicated by the vertical line $t_0 + N_1 T_s$, with T_s being the sampling interval. Within the time interval $[t_0; t_0 + N_1 T_s]$, the calculated command sequence $\hat{U}$ is optimal concerning the criterion. However, the satisfaction of the inequality constraints can be ensured over a much longer interval $[t_0; t_0 + (N_1 + N_2)T_s]$. The gray shadings before time t and after time $t_0 + (N_1 + N_2)T_s$ show the areas which are not subject to optimization, that is, there is no knowledge about the inputs or outputs outside the interval $[t_0; t_0 + (N_1 + N_2)T_s]$.

What is finally done with the calculated command sequence $\hat{U}$? Only the first element of $\hat{U}$ is applied, that is, fed into the control effector suite. Afterwards, the line separating past and future moves ahead by one sampling interval, that is, t_0 increases by T_s (illustrated by the big arrow in Fig. 7). At this new point, the whole optimization problem is solved again. This is why this method is also referred to as receding-horizon control.

B. Expression of the Controlled Outputs

This section addresses the problem of finding a mathematical formulation for the control allocation problem. The aim, described in the Introduction, is to track the flight dynamics outputs as closely as possible, while imposing amplitude constraints on a certain structural load output. Thus, the output vector has to be separated into output signals subject to tracking performance y_t and output signals subject to amplitude constraints y_c:

$$y = \begin{bmatrix} y_t \\ y_c \end{bmatrix} \quad \text{with } y_t \in \mathbb{R}^{p_t}, \qquad y_c \in \mathbb{R}^{p_c}$$

The discretization of the A/C model using the sampling interval T_s yields the following equations:

$$(\mathbf{S}) \begin{cases} x^{(k+1)} = Ex^{(k)} + Fu^{(k)} & \text{with } u \in \mathbb{R}^m; \qquad x \in \mathbb{R}^n \\ \begin{bmatrix} y_t^{(k)} \\ y_c^{(k)} \end{bmatrix} = \begin{bmatrix} G_t \\ G_c \end{bmatrix} x^{(k)} \end{cases} \tag{1}$$

Furthermore, the simulation horizon for the tracking output is denoted N_1 (cf. Fig. 7). For the moment, the simulation horizon for the output constraint requirements is N_1 as well.

The output reference trajectory, which is the trajectory to be tracked as closely as possible, is then given in the form of a vector $Y_{t,\text{ref}}$ which contains the vectors $y_{t,\text{ref}}^{(k)}$ at all sampling points $k = 2, \ldots, (N_1 + 1)$. The same is true for the output trajectory Y_t. The difference is that the latter is yet unknown, whereas the reference trajectory has been obtained in a simulation. The constrained outputs and the command reference trajectory can be represented in the same way [see Eq. (2)]. Again, these are yet unknown and have to be determined in the subsequent optimization.

$$Y_{t,\mathrm{ref}} = \begin{bmatrix} y_{t,\mathrm{ref}}^{(2)} \\ y_{t,\mathrm{ref}}^{(3)} \\ \vdots \\ y_{t,\mathrm{ref}}^{(N_1)} \\ y_{t,\mathrm{ref}}^{(N_1+1)} \end{bmatrix}, \qquad Y_t = \begin{bmatrix} y_t^{(2)} \\ y_t^{(3)} \\ \vdots \\ y_t^{(N_1)} \\ y_t^{(N_1+1)} \end{bmatrix}, \qquad Y_c = \begin{bmatrix} y_c^{(2)} \\ y_c^{(3)} \\ \vdots \\ y_c^{(N_1)} \\ y_c^{(N_1+1)} \end{bmatrix}, \qquad U = \begin{bmatrix} u^{(1)} \\ u^{(2)} \\ \vdots \\ u^{(N_1-1)} \\ u^{(N_1)} \end{bmatrix} \tag{2}$$

The vectors Y_t and Y_c can be expressed in a function of the (unknown) command sequence U. Indeed, when applied to the whole horizon N_1, the recurrence relation given by the state equation (1) gives these relations:

$$\underbrace{\begin{bmatrix} y_t^{(2)} \\ y_t^{(3)} \\ \vdots \\ y_t^{(N_1)} \\ y_t^{(N_1+1)} \end{bmatrix}}_{Y_t} = \underbrace{\begin{bmatrix} G_tF & 0 & \cdots & 0 & 0 \\ G_tEF & G_tF & \cdots & 0 & 0 \\ \vdots & \vdots & \ddots & \vdots & \vdots \\ G_tE^{N_1-2}F & G_tE^{N_1-3}F & \cdots & G_tF & 0 \\ G_tE^{N_1-1}F & G_tE^{N_1-2}F & \cdots & G_tEF & G_tF \end{bmatrix}}_{\mathcal{H}_t} \underbrace{\begin{bmatrix} u^{(1)} \\ u^{(2)} \\ \vdots \\ u^{(N_1-1)} \\ u^{(N_1)} \end{bmatrix}}_{U} + \underbrace{\begin{bmatrix} G_tE \\ G_tE^2 \\ \vdots \\ G_tE^{N_1-1} \\ G_tE^{N_1} \end{bmatrix}}_{\mathcal{G}_t} x^{(1)}$$

$$\underbrace{\begin{bmatrix} y_c^{(2)} \\ y_c^{(3)} \\ \vdots \\ y_c^{(N_1)} \\ y_c^{(N_1+1)} \end{bmatrix}}_{Y_c} = \underbrace{\begin{bmatrix} G_cF & 0 & \cdots & 0 & 0 \\ G_cEF & G_cF & \cdots & 0 & 0 \\ \vdots & \vdots & \ddots & \vdots & \vdots \\ G_cE^{N_1-2}F & G_cE^{N_1-3}F & \cdots & G_cF & 0 \\ G_cE^{N_1-1}F & G_cE^{N_1-2}F & \cdots & G_cEF & G_cF \end{bmatrix}}_{\mathcal{H}_c} \underbrace{\begin{bmatrix} u^{(1)} \\ u^{(2)} \\ \vdots \\ u^{(N_1-1)} \\ u^{(N_1)} \end{bmatrix}}_{U} + \underbrace{\begin{bmatrix} G_cE \\ G_cE^2 \\ \vdots \\ G_cE^{N_1-1} \\ G_cE^{N_1} \end{bmatrix}}_{\mathcal{G}_c} x^{(1)}$$

Or, in a shorter notation:

$$Y_t = \mathcal{G}_t \cdot x^{(1)} + \mathcal{H}_t \cdot U \quad \text{and} \quad Y_c = \mathcal{G}_c \cdot x^{(1)} + \mathcal{H}_c \cdot U \tag{3}$$

The respective expressions for the tracking and constrained outputs are thus linear w.r.t. the command sequence vector U.

C. Formulation of the Criterion

A formulation using the 2-norm (Cartesian norm) is chosen to describe the tracking requirement in a mathematical form:

$$\min_U J = \|Y_t - Y_{t,\mathrm{ref}}\|_2 \tag{4}$$

The solution

$$\hat{U} = \arg\min_U J$$

is the command sequence resulting in the least-squares error between the reference output sequence $Y_{t,\mathrm{ref}}$ and the optimized output sequence Y_t. The evaluation of Eq. (4) using Eq. (3) yields the following expression:

$$\begin{aligned} \min_U J = {} & U^T\mathcal{H}_t^T\mathcal{H}_tU + U^T\mathcal{H}_t^T\mathcal{G}_tx^{(1)} - U^T\mathcal{H}_t^TY_{t,\mathrm{ref}} + x^{(1)T}\mathcal{G}_t^T\mathcal{H}_tU \\ & - Y_{t,\mathrm{ref}}^T\mathcal{H}_tU - Y_{t,\mathrm{ref}}^T\mathcal{G}_tx^{(1)} + x^{(1)T}\mathcal{G}_t^T\mathcal{G}_tx^{(1)} + Y_{t,\mathrm{ref}}^TY_{t,\mathrm{ref}} \\ & - x^{(1)T}\mathcal{G}_t^TY_{t,\mathrm{ref}} \end{aligned}$$

Or, in a shorter notation:

$$\begin{gathered} J = U^T\mathcal{H}_t^T\mathcal{H}_tU + a^TU + d \quad \text{with } a^T = 2x^{(1)T}\mathcal{G}_t^T\mathcal{H}_t - 2Y_{t,\mathrm{ref}}^T\mathcal{H}_t \\ d = (\mathcal{G}_tx^{(1)} - Y_{t,\mathrm{ref}})^T(\mathcal{G}_tx^{(1)} - Y_{t,\mathrm{ref}}) \end{gathered} \tag{5}$$

D. Formulation of the Constraints

1) As a first constraint, the deflection angle of each control effector has a superior and an inferior bound, to be respected at each point of time $t_0 + kT_s$, where T_s denotes the sampling interval:

$$u_{\min} \le u^{(k)} \le u_{\max}, \qquad k = 1, \ldots, N_1 \qquad u_{\min}, u_{\max} \in \mathbb{R}^m$$

Here, the inequality sign is supposed to be understood componentwise, that is, $u_{\min}$ and $u_{\max}$ contain the lower and upper limits for each control effector, respectively.

If this representation is expanded to the horizon of the simulation, $k = 1, \ldots, N_1$, the following relation is obtained, where I is the identity matrix of size $(N_1 \cdot m) \times (N_1 \cdot m)$:

$$U_{\min} = \begin{bmatrix} u_{\min} \\ \vdots \\ u_{\min} \end{bmatrix} \le I \cdot U \le \begin{bmatrix} u_{\max} \\ \vdots \\ u_{\max} \end{bmatrix} = U_{\max} \tag{6}$$

2) A similar expression can be obtained for the actuator rates:

$$\begin{gathered} \Delta u_{\min} \le \Delta u^{(k)} \le \Delta u_{\max}, \qquad k = 1, \ldots, N_1 \\ \Delta u_{\min}, \Delta u_{\max} \in \mathbb{R}^m \end{gathered}$$

Here, $\Delta u_{\min}$ and $\Delta u_{\max}$ contain the minimum and maximum angular velocities for each control effector, respectively. This inequality is expanded to the horizon of the simulation as follows:

$$\Delta U_{\min} = \begin{bmatrix} \Delta u_{\min} \\ \vdots \\ \Delta u_{\min} \end{bmatrix} \le \Delta U \le \begin{bmatrix} \Delta u_{\max} \\ \vdots \\ \Delta u_{\max} \end{bmatrix} = \Delta U_{\max} \tag{7}$$

where

$$\Delta U = \begin{bmatrix} \Delta u^{(1)} \\ \Delta u^{(2)} \\ \vdots \\ \Delta u^{(N_1-1)} \\ \Delta u^{(N_1)} \end{bmatrix} = \begin{bmatrix} u^{(1)} - u^{(0)} \\ u^{(2)} - u^{(1)} \\ \vdots \\ u^{(N_1-1)} - u^{(N_1-2)} \\ u^{(N_1)} - u^{(N_1-1)} \end{bmatrix}$$

$$= \underbrace{\begin{bmatrix} I & 0 & \cdots & 0 & 0 \\ -I & I & \cdots & 0 & 0 \\ \vdots & \vdots & \ddots & \vdots & \vdots \\ 0 & 0 & \cdots & I & 0 \\ 0 & 0 & \cdots & -I & I \end{bmatrix}}_{N} \begin{bmatrix} u^{(1)} \\ u^{(2)} \\ \vdots \\ u^{(N_1-1)} \\ u^{(N_1)} \end{bmatrix} - \underbrace{\begin{bmatrix} u^{(0)} \\ 0 \\ \vdots \\ 0 \\ 0 \end{bmatrix}}_{b} = N \cdot U - b$$

and where $u^{(0)}$ is the most recent command vector in the past (the command vector which has just been applied).

3) The last constraint concerns the structural load output. Similarly to what has been said about the control effector amplitude constraints, the constrained output $y_c^{(k)}$ must be within an admissible interval at each point of time $t_0 + kT_s$:

$$y_{c,\min} \le y_c^{(k)} \le y_{c,\max}, \qquad k = 2, \ldots, N_1 + 1$$
$$y_{c,\min}, y_{c,\max} \in \mathbb{R}^{p_c}$$

Formulating this for the whole interval and resorting to Eq. (3) yields

$$Y_{c,\min} = \begin{bmatrix} y_{c,\min} \\ y_{c,\min} \\ \vdots \\ y_{c,\min} \\ y_{c,\min} \end{bmatrix} \le \mathcal{H}_c \cdot U + \mathcal{G}_c \cdot x^{(1)} \le \begin{bmatrix} y_{c,\max} \\ y_{c,\max} \\ \vdots \\ y_{c,\max} \\ y_{c,\max} \end{bmatrix} = Y_{c,\max} \tag{8}$$

The combination of the three types of constraints (amplitude constraints of the control effectors [Eq. (6)], rate constraints of the control effectors [Eq. (7)], and amplitude constraints of the structural load output [Eq. (8)]) in one single expression leads to

$$H \cdot U \le c \quad \text{with } H = \begin{bmatrix} I \\ -I \\ \mathcal{H}_c \\ -\mathcal{H}_c \\ N \\ -N \end{bmatrix} \quad \text{and}$$
$$c = \begin{bmatrix} U_{\max} \\ -U_{\min} \\ Y_{c,\max} - \mathcal{G}_c \cdot x^{(1)} \\ -Y_{c,\min} + \mathcal{G}_c \cdot x^{(1)} \\ \Delta U_{\max} + b \\ -\Delta U_{\min} - b \end{bmatrix} \tag{9}$$

E. Numerical Solution

In the previous section the control allocation problem is mathematically formulated as a constrained quadratic programming problem (QP):

$$\min_U J = U^T \mathcal{H}_t^T \mathcal{H}_t U + a^T U + d \qquad \text{such that } H \cdot U \le c$$

The constant term d in the criterion can be ignored. It can be shown that the Hessian matrix $\mathcal{H}_t^T \mathcal{H}_t$ is a positive definite matrix, that is, it is symmetric and all its eigenvalues are positive. In addition, all constraints are linearly expressed in U. These two properties yield a special type of QP problem, a convex QP problem (CQP). There exists a special algorithm capable of dealing with this problem very efficiently, the algorithm of Goldfarb and Idnani. This method belongs to the active-set methods and works on the primal and dual formulation of the problem [18,19]. The algorithm used in this application is the one delivered in FORTRAN 77.[§] The formulation of the whole problem in MATLAB made the implementation of an interface and various changes in the FORTRAN code necessary. This effort pays off when the calculation time needed by the FORTRAN implementation is compared with the one needed by the standard MATLAB function "quadprog."

Unfortunately, difficulties usually arise with matrices of great size. Although in theory, the Hessian matrix is positive definite, this is not the case for the numerical model used in MATLAB. Round-off errors are necessarily introduced into the model due to finite machine precision. This can lead to a Hessian matrix which is practically positive semidefinite (ill conditioned), that is, the condition number is very high, for example, on the order of 10^{20}. This makes the use of the algorithm of Goldfarb and Idnani impossible. This phenomenon depends on the input data and does not always occur.

There is a simple way to solve this problem. Instead of using $\mathcal{H}_t$, the Hessian matrix is computed with an extension of $\mathcal{H}_t$ in the following way:

$$\tilde{\mathcal{H}}_t = \begin{bmatrix} \mathcal{H}_t \\ \varepsilon_1 M \end{bmatrix}$$

The matrix M is square, and it has to be ensured that M has no eigenvalues near zero. This requirement is necessary to cure the semidefiniteness of the Hessian matrix. Rewriting the whole optimization criterion using $\tilde{\mathcal{H}}_t$ instead of $\mathcal{H}_t$ yields the following expression:

$$\tilde{J} = U^T \tilde{\mathcal{H}}_t{}^T \tilde{\mathcal{H}}_t U + \tilde{a}^T U + \tilde{d} = J + \varepsilon_1^2 U^T M^T M U$$

One possibility for the choice of M is straightforward:

$$M_1 = I \Rightarrow \tilde{J} = J + \varepsilon_1^2 U^T U$$

This corresponds to a weighting imposed on the command sequence U, that is, the total energy invested into control action is penalized.

A slightly more subtle choice of M means that the rates of the control effectors ΔU are penalized:

$$\left.\begin{array}{c} M_2 = N \ \text{[defined in Eq. (8)]} \\ \tilde{a}^T = a^T - 2\varepsilon_1^2 b^T N \\ \tilde{d} = d + \varepsilon_1^2 b^T b \end{array}\right\} \Rightarrow \tilde{J} = U^T \tilde{\mathcal{H}}_t^T \tilde{\mathcal{H}}_t U + \tilde{a}^T U + \tilde{d}$$
$$= J + \varepsilon_1^2 \Delta U^T \Delta U$$

These two additional weightings give the possibility to cure the problem of ill-conditioned Hessian matrices while still having a physical sense behind the actions taken. In any case, ε_1 should be chosen very small, for example, on the order of 10^{-6}, in order not to disturb the actual optimization criterion too much.

IV. Extensions and Application to the A/C Model

A. Soft Constraints

In special cases, there does not exist any solution to the QP problem. This means that the set within the inequality constraints is empty, that is, there exists no command sequence which respects the constraints on the structural load output. To prevent this from happening, the three types of constraints [formulated in the form of hard constraints in Eq. (9)] become soft constraints:

$$H \cdot U \le c + \lambda \cdot \mathcal{I} \quad \text{or} \quad [H \quad -\mathcal{I}] \cdot \begin{bmatrix} U \\ \lambda \end{bmatrix} \le c$$

$\mathcal{I}$ is the column vector consisting of ones. λ is a scalar slack variable.

[§]Spellucci, P., Moderne Methoden der linearen und nichtlinearen Optimierung—Vorlesungsskript SS 2000, Technische Universität Darmstadt, FB Mathematik, 2000, available at http://www.mathematik.tudarmstadt.de:8080/ags/ag8/Mitglieder/spellucci/docs/optiss2000.ps.gz [retrieved June 2003].

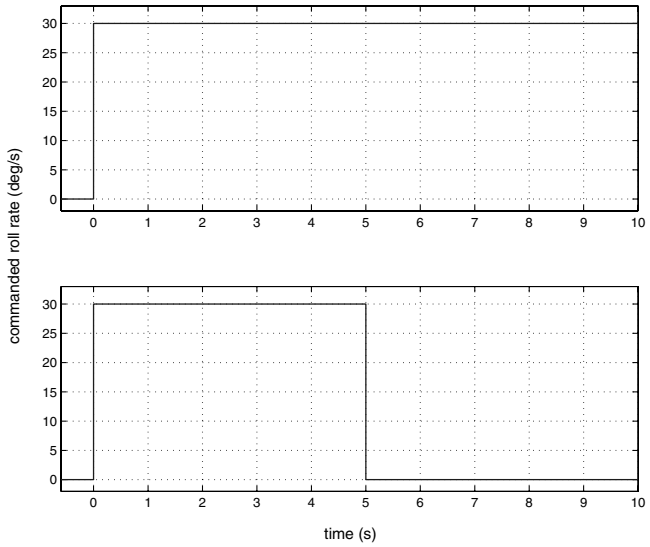

Fig. 8 Solution to the causality problem.

The optimization criterion given in Eq. (5) has to be rewritten in the following form:

$$\bar{J} = \begin{bmatrix} U \\ \lambda \end{bmatrix}^T \begin{bmatrix} \mathcal{H}_t & 0 \\ 0 & \varepsilon_2 \end{bmatrix}^T \begin{bmatrix} \mathcal{H}_t & 0 \\ 0 & \varepsilon_2 \end{bmatrix} \begin{bmatrix} U \\ \lambda \end{bmatrix} + \begin{bmatrix} a \\ 0 \end{bmatrix}^T \begin{bmatrix} U \\ \lambda \end{bmatrix} + d = J + \varepsilon_2^2 \lambda^2$$

Clearly, λ is now a part of the optimization vector $[\,U^T \quad \lambda\,]^T$ and the criterion $\bar{J}$. The aim is to push λ as close as possible to zero. At the end of the optimization, λ will necessarily have a positive value. To prioritize the constraints, it is necessary to choose a big value for ε_2, for example, on the order of 10^{10}. For feasible problems, it is then usual for λ to be on the order of 10^{-20}.

B. Extended Constraint Handling

The idea is to incorporate the structural load output constraint over a longer interval ($[1; N_1 + N_2]$) than the output tracking ($[1; N_1]$) (see Fig. 7). The command sequence is supposed to be constant in the interval $[N_1; N_1 + N_2]$, assuming the value from the point of time N_1. It is not necessary to reformulate the control effector saturations, because they are automatically satisfied. This extension of the constraint handling yields much better results when the constraint imposed on the structural load output is very strict.

C. Causality

Because of the predictive nature of the MPC method, the algorithm has access to future values of the reference trajectory $Y_{t,\mathrm{ref}}$. This means that there is a possibility for the algorithm to anticipate the pilot's future stick and pedal inputs.

The most straightforward cure would be to only give the controller as much information concerning the pilot's actions as is available at the present time. Figure 8 shows how this can be done for the reference maneuver shown in Fig. 6. The upper curve shows the reference maneuver known to the MPC algorithm in the interval [0;5 s]. The lower curve contains the values known after the time 5 s. Thus two sets of reference trajectories are generated. At the time 5 s, the algorithm switches from the first to the second set.

D. Application to the Flexible A/C Model

This simulation makes use of the five main control effectors (ailerons, elevators, and rudder). The aim is to show that it is possible to guarantee upper and lower bounds on the structural load output M_x of 500,000 and $-500,000$ Nm respectively. Table 1 details the settings used in this test case. Figure 9 then compares the control effector inputs and the structural load output M_x for the reference simulation (solid lines) and the simulation with MPC (dashed lines).

Table 1 Optimization settings for the simulation using the five main control effectors

Name	Symbol	Value
Optimization horizon	N_1	32
Additional constraint horizon	N_2	50
Penalized variable		ΔU
Weighting for penalization	ε_1	0.10
Constraint handling		Soft
Constraint noncompliance penalization	ε_2	1.00×10^{10}
Constrained output		M_x external wing
Constraint limits	$M_{x,\max}$	$+500,000$ Nm
	$M_{x,\min}$	$-500,000$ Nm
Causality ensured		Yes

The optimization horizon of 32 steps has shown to be sufficient to yield satisfactory results. A slight weighting on the variable ΔU is absolutely necessary in this case to guarantee numerical convergence, due to the fact that the problem is redundant using all five main control surfaces for the lateral control of the A/C. To give an impression of the size of the problem, the Hessian $\tilde{\mathcal{H}}_t^T \tilde{\mathcal{H}}_t$ has the dimensions 160×160.

All constraints are fulfilled. The amplitude constraints of the control effectors are respected, and their rate constraints can be seen in the ramp behavior in some areas. The structural load limit is obviously achieved by removing a part of the ARW and ALW control action and adding it to RE, LE, and RR. It can, in particular, be seen that the elevators, which are usually dedicated to the longitudinal control of the A/C, bring here a significant contribution to the lateral control, due to their antisymmetric behavior.

Finally, the flight behavior is preserved because the flight dynamics outputs are perfectly tracked. Indeed, the simulation with MPC can hardly be distinguished from the reference simulation, and thus it is not shown here.

V. Synthesis of the New Mixing Unit

Let $\tilde{U}$ be the optimal sequence of control effector inputs $\tilde{u}$ obtained at the end of Sec. IV and plotted in Fig. 9. The computation of $\tilde{U}$ is usually referred to as the analysis phase. Strictly speaking, no controller synthesis is performed at this stage. The aim of this section is now to synthesize a new mixing law that is able to reproduce this optimal sequence.

More precisely, an open-loop simulation of the A/C model and the nominal controller is first performed to obtain the optimal sequence $\tilde{V}$ of controller outputs $\tilde{v}$, as depicted in Fig. 10. The issue is then to identify the new mixing unit knowing its input and output sequences $\tilde{V}$ and $\tilde{U}$, cf. Fig. 11.

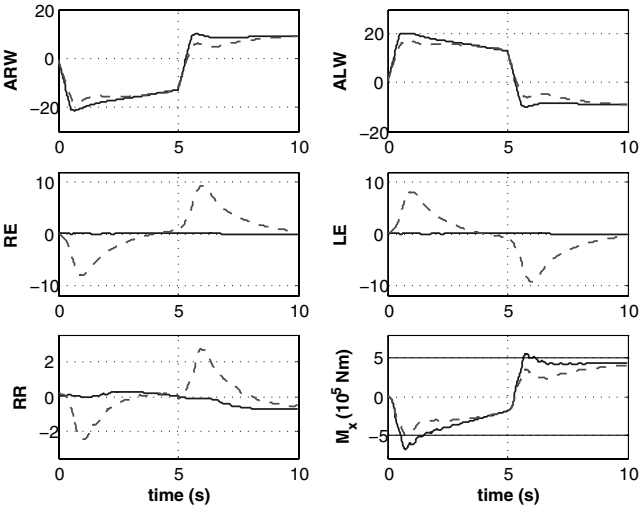

Fig. 9 Simulations using the five main control effectors.

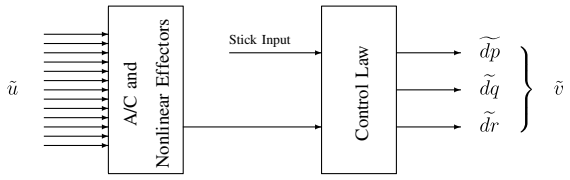

Fig. 10 Open-loop simulation of the A/C model.

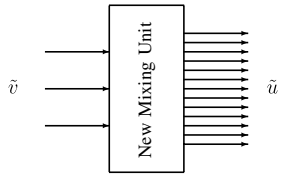

Fig. 11 Identification of the new mixing unit.

The idea is to perform the identification in the frequency domain by minimizing a nonlinear criterion. This method is theoretically simple but requires one to make a priori strong assumptions, yet not too restrictive for the considered identification issue, on the structure of the mixing unit.

A. Preliminary Assumptions

The mixing unit is first segregated into several single-input/single-output (SISO) subsystems to be identified separately. Each of these subsystems is associated to a specific control effector and only exploits the input signal $\widetilde{dp}$, while $\widetilde{dq}$ and $\widetilde{dr}$ are ignored.

Several major arguments justify the choice of this SISO limitation. From a qualitative point of view, the reference scenario is a sudden and strong roll maneuver (see Sec. II.D), which suggests to favor the movement around the roll axis. Although it seems quite obvious to associate the control effectors usually involved in the lateral movement of the A/C (ailerons and rudder) to the input signal $\widetilde{dp}$, it seems more difficult to do the same with the elevators. Nevertheless, the shape of the optimal curves plotted in Fig. 9 clearly indicates that the elevators, similarly to the ailerons, have an antisymmetric behavior that allows one to alleviate the structural load at the external wing. More quantitatively, the maximal amplitude of $\widetilde{dp}$ is about 20 deg/s, while $\widetilde{dq}$ and $\widetilde{dr}$ remain less than 0.3 deg/s, which reinforces the aforementioned assumption.

Furthermore, it is assumed that each of the SISO subsystems is composed of the following parts:

1) a delay block,

2) a continuous-time transfer function,

3) saturations corresponding to the amplitude and rate constraints of the considered control effector.

This second assumption is justified by the selected identification method that allows one to identify a SISO transfer function, but also by the observation of the optimal curves plotted in Fig. 9, which highlight delays and saturations. The structure of such a subsystem is depicted in Fig. 12.

B. Identification Method

This section presents a method to identify a fixed-order SISO continuous-time transfer function from time-domain data. It consists of three successive steps:

1) computation of the impulse response by solving a least-squares problem,

2) computation of the frequency response by Fourier discrete transform,

3) identification of the transfer function by minimizing a nonlinear criterion.

1. Computation of the Impulse Response

Let $(\tilde{v}^{(k)})_{k\in[1,N_s]}$ and $(\tilde{u}^{(k)})_{k\in[1,N_s]}$ be the N_s input and output time-domain samples available for identification. It is assumed that $\tilde{v}^{(k)} = 0$ and $\tilde{u}^{(k)} = 0$ for $k \notin [1, N_s]$. The issue is to compute the N first coefficients $(g^{(k)})_{k\in[1,N]}$ of the impulse response G by minimizing the following quadratic criterion:

$$J(G) = \frac{1}{2}\sum_{j=1}^{N_s}\left(\tilde{u}^{(j)} - \sum_{k=1}^{N} g^{(k)}\tilde{v}^{(j-k+1)}\right)^2 \tag{10}$$

The solution of this least-squares problem is obtained by solving the linear system $\partial J/\partial g^{(i)} = 0$ for $i = 1, \ldots, N$ with

$$\frac{\partial J}{\partial g^{(i)}} = -\sum_{j=1}^{N_s}\tilde{v}^{(j-i+1)}\left(\tilde{u}^{(j)} - \sum_{k=1}^{N} g^{(k)}\tilde{v}^{(j-k+1)}\right) = 0 \tag{11}$$

so as to obtain the following matrix representation, from which the computation of G is straightforward:

$$A \cdot G = B, \qquad A \in \mathbb{R}^{N\times N}, \qquad B \in \mathbb{R}^{N\times 1} \tag{12}$$

$$A = \begin{pmatrix} \sum_{j=1}^{N_s}(\tilde{v}^{(j)})^2 & \cdots & \sum_{j=1}^{N_s}\tilde{v}^{(j)}\tilde{v}^{(j-N+1)} \\ \vdots & \ddots & \\ \sum_{j=1}^{N_s}\tilde{v}^{(j-N+1)}\tilde{v}^{(j)} & & \sum_{j=1}^{N_s}(\tilde{v}^{(j-N+1)})^2 \end{pmatrix}$$

$$B = \begin{pmatrix} \sum_{j=1}^{N_s}\tilde{v}^{(j)}\tilde{u}^{(j)} \\ \vdots \\ \sum_{j=1}^{N_s}\tilde{v}^{(j-N+1)}\tilde{u}^{(j)} \end{pmatrix}$$

A direct inversion of the A matrix often leads to a noisy impulse response that is not suitable for identification purposes. To obtain a smoother response, it is first possible to perform a singular value decomposition of the A matrix so as to keep only the n highest singular values, with $n < N$.

2. Computation of the Frequency Response

Let T_s be the previously defined sampling period and N_0 be a given integer. The frequency response $\mathbf{G}$ on the interval $[0, \frac{\pi}{T_s}[$ and with a sampling interval $\Delta\omega = \frac{\pi}{N_0 T_s}$ is directly obtained as the discrete Fourier transform of the impulse response G as follows:

$$\mathbf{G}(j\omega_i) = \sum_{k=1}^{N} g^{(k)} e^{-j\omega_i T_s(k-1)}, \qquad \omega_i = \frac{\pi(i-1)}{N_0 T_s} \qquad i = 1, \ldots, N_0 \tag{13}$$

3. Identification of the Transfer Function

In the third step, the aim is to convert the discrete frequency response $\mathbf{G}(j\omega_i)$ computed at frequencies ω_i, for $i = 1, \ldots, N_0$, into a rational transfer function $\mathbf{F}(p)$ defined by

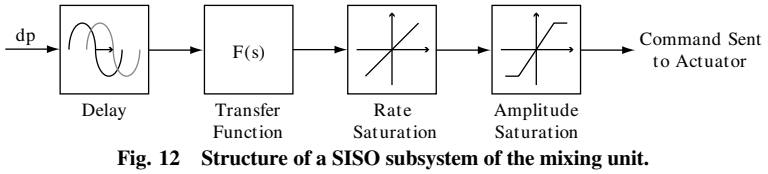

Fig. 12 Structure of a SISO subsystem of the mixing unit.

$$\mathbf{F}(p) = \frac{\mathbf{N}(p)}{\mathbf{D}(p)} = \frac{a_0 + a_1 p + \cdots + a_\alpha p^\alpha}{1 + b_1 p + \cdots + b_\beta p^\beta} \tag{14}$$

Let $X = (a_0 \cdots a_\alpha \; b_1 \cdots b_\beta)^T$ be the optimization parameters. The issue is to compute

$$\hat{X} = \arg\min_X J(X)$$

where the error criterion $J(X)$ is defined as follows:

$$J(X) = \sum_{i=1}^{N_f} \frac{1}{\omega_i} \left| \mathbf{G}(j\omega_i) - \frac{\mathbf{N}(j\omega_i)}{\mathbf{D}(j\omega_i)} \right|^2 \tag{15}$$

The introduction of weighting factors $\frac{1}{\omega_i}$ allows one to favor low frequencies in the criterion. It is important to remember that the outputs of the mixing unit correspond to commands sent to the control effectors, whose behavior can be assimilated to low-pass filters with relatively low cutoff frequencies. In the same perspective, N_f is a tuning parameter which is lower than N_0 and allows one to perform the identification on the reduced frequency interval $[0, \pi(N_f - 1)/N_0 T_s]$.

$J(X)$ is a nonlinear criterion due to the optimization parameters $b_1, \ldots, b_\beta$ in $\mathbf{D}(p)$. The idea to tackle this drawback is to replace this nonlinear criterion by a sequence of linear criteria $J_k(X_k)$, as proposed by Sanathanan and Koerner [16]:

$$J_k(X_k) = \sum_{i=1}^{N_f} \frac{1}{\omega_i} \frac{1}{|\mathbf{D}_{k-1}(j\omega_i)|^2} |\mathbf{D}_k(j\omega_i)\mathbf{G}(j\omega_i) - \mathbf{N}_k(j\omega_i)|^2 \tag{16}$$

Minimizing J_k consists of solving the following linear system in the least-squares sense, where Re and Im denote the real and imaginary parts of a complex number, respectively:

$$\begin{cases} \frac{1}{\omega_i} \frac{1}{|\mathbf{D}_{k-1}(j\omega_i)|} \{\mathrm{Re}[\mathbf{D}_k(j\omega_i)\mathbf{G}(j\omega_i)] - Re[\mathbf{N}_k(j\omega_i)]\} = 0 \\ \frac{1}{\omega_i} \frac{1}{|\mathbf{D}_{k-1}(j\omega_i)|} \{\mathrm{Im}[\mathbf{D}_k(j\omega_i)\mathbf{G}(j\omega_i)] - Im[\mathbf{N}_k(j\omega_i)]\} = 0 \end{cases} \tag{17}$$

This system can be equivalently rewritten in a more concise form:

$$A_k X_k = B_k, \qquad X_k = (a_{0k} \cdots a_{\alpha k} b_{1k} \cdots b_{\beta k})^T$$
$$A_k \in \mathbb{R}^{2N_f \times (\alpha+\beta+1)}, \qquad B_k \in \mathbb{R}^{2N_f \times 1}$$

and the optimal solution in the least-squares sense can be easily obtained using the Moore–Penrose pseudoinverse $A_k^\dagger$:

$$X_k = A_k^\dagger B_k \tag{18}$$

At iteration number k, the transfer function parameters X_k are thus calculated from the minimization of the linear least-squares criterion J_k, which itself depends on the parameter values X_{k-1} computed at the previous iteration. This iterative procedure can be initialized with $\mathbf{D}_0(p) = 1$.

This approach should be handled carefully, because the asymptotic nature of a sequence of error criteria does not determine the asymptotic nature of their minimizing solutions. It can indeed be shown that X_k does not necessarily tend asymptotically to the solution X of the fundamental nonlinear least-squares criterion (15), even though the sequence of error criteria J_k tends asymptotically to the nonlinear least-squares criterion.

However, numerical implementation in [20] has shown that, when convergent, the identification scheme of Sanathanan and Koerner can produce satisfactory fits to frequency-response data. This assumes that the data are comparatively noise free, which is here a reasonable assumption.

If the results prove unsatisfactory, some alternative sequences of linear criteria exist to generate solutions X_k that tend asymptotically to the solution of the initial nonlinear least-squares criterion [17].

C. Computational Aspects and Results

This method has been implemented and applied to identify the new mixing unit. As shown in Sec. IV.D, the five main control effectors (ailerons, elevators, and rudder) are sufficient to achieve the structural load limit, so the spoilers are not taken into account.

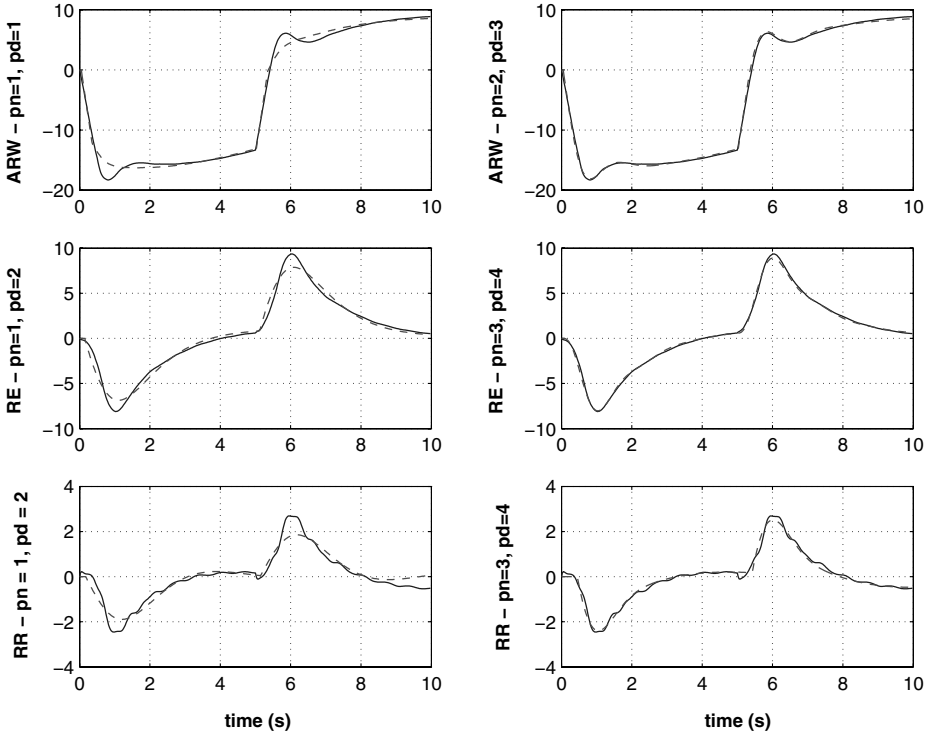

Fig. 13 Open-loop identification of the control effector inputs.

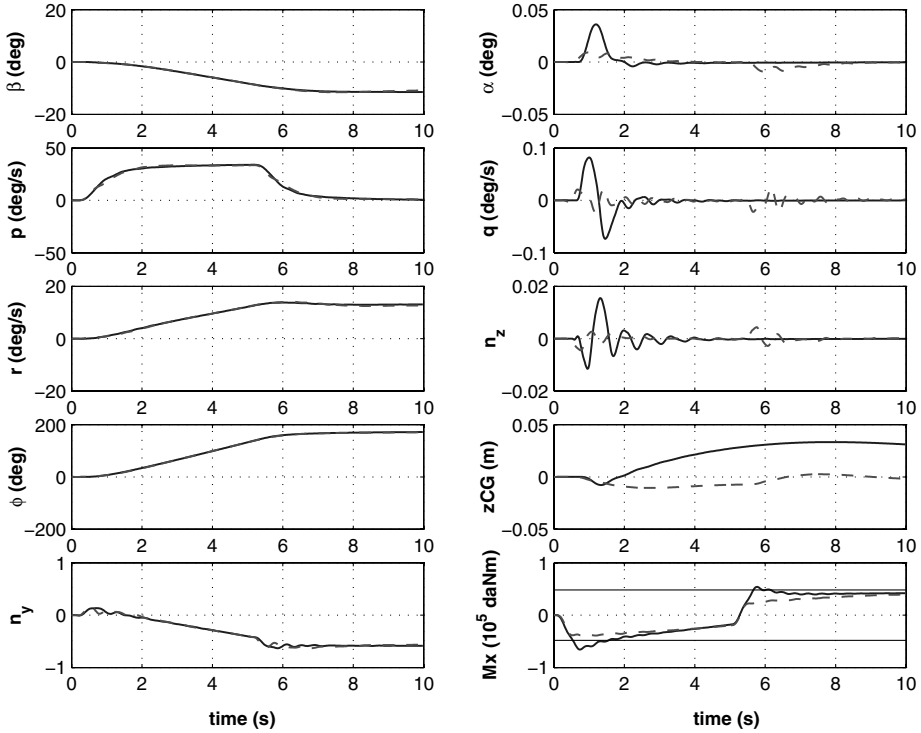

Fig. 14 Closed-loop simulations with the reference and the identified mixing units.

1. Open-Loop Identification

Five subsystems, associated with each of the considered control effectors, are identified using the time-domain data computed at the end of Sec. IV and following the method described in Sec. V.B.

Figure 13 shows the results for ARW, RE, and RR. The optimal and the identified control effector inputs are plotted as solid and dashed lines, respectively. In each case, both low-order (left plots) and high-order (right plots) transfer functions are identified, where pn and pd denote the orders of the numerator and the denominator, respectively.

If the orders of the identified transfer functions are sufficiently high (right plots), the results prove to be excellent, because the optimal and the identified curves are almost identical in all cases. Unfortunately, this leads to a rather complex mixing unit, which is not desirable from a practical viewpoint.

But the most important point is the closed-loop behavior of the A/C, that is, limiting the amplitude of the structural load at the external wing while keeping the flight behavior as close as possible to the initial one. The idea therefore consists of choosing appropriate low-order transfer functions (left plots) that guarantee an adequate closed-loop behavior, even if the open-loop identification appears less accurate.

2. Closed-Loop Simulation

Following this strategy, the total order of the new mixing unit is 8. Table 2 details the settings used for the identification process and the main characteristics of the resulting mixing unit. Note that for all subsystems, $N_0 = 10^5$ and the length of the impulse response N is equal to the number of time-domain samples N_s, so these parameters are not included in Table 2.

Figure 14 then compares the flight dynamics and the structural load outputs when the reference (solid lines) or the identified (dashed lines) mixing unit is implemented. The lateral flight parameters β, p, r, ϕ, and n_y are perfectly tracked and the constraint on the structural load M_x is fulfilled, which demonstrates the efficiency of the identification scheme.

A purely lateral maneuver is considered and the longitudinal flight parameters α, q, n_z, and z_{CG} only vary because of the small coupling between the longitudinal and the lateral motions of the A/C. Moreover, these variations do not affect the A/C behavior, provided that their amplitude remains very low. Consequently, it is useless to perform an exact tracking, and the new mixing unit should just ensure that the longitudinal flight parameters keep the same magnitude, which is obviously the case here.

The A/C closed-loop behavior is hence very satisfactory, and the identification procedure is also relevant because:

1) the complexity of the new mixing unit remains moderate, and

2) its structure keeps a physical meaning, which is a common desire in industrial applications.

VI. Conclusions

A new mixing law for a flexible transport aircraft is designed in this paper. This law allows one to alleviate the bending moment at the external wing during a sudden and strong roll maneuver, while respecting the nominal flight behavior. The capability of model predictive control to deal explicitly with given time-domain constraints and criteria makes this method particularly adapted to the

Table 2 Identification settings and characteristics of the new mixing unit

Control effector	ARW	ALW	RE	LE	RR
Delay, s	0	0	0.1	0.1	0.125
Number of time-domain samples (N_s)	320	320	361	366	315
Number of singular values (n)	15	19	17	17	11
Number of frequency points (N_f)	900	900	2500	2500	1800
Order of the numerator (pn)	1	1	1	1	1
Order of the denominator (pd)	1	1	2	2	2

considered control allocation problem. It can indeed generate an optimal sequence of control effector inputs offline, complying with the control effector saturations as well as the constrained load output and the tracked flight dynamics outputs. A mixing unit is then synthesized using a frequency-domain identification method. The new mixing unit performs well because the control effector inputs sequence can be precisely reproduced using only low-order transfer functions. As a result, all load alleviation and tracking objectives are fulfilled, and the complexity of the resulting mixing strategy remains moderate, which demonstrates the efficiency of the design scheme. Additional tests showed that an even more tightened constraint on the structural load—without modifying the flight dynamics outputs—can be achieved using the spoilers in the design process.

The identification step could be further improved to deal with more complex maneuvers, for which the SISO limitation is too restrictive. Extending the proposed method to the multi-input/multi-output (MIMO) case is thinkable, yet not straightforward. State-space approaches based on subspace identification also appear promising.

Acknowledgment

This work was supported by DPAC (Direction des Programmes de l'Aviation Civile) and Airbus France.

References

[1] Virnig, J. C., and Bodden, D. S., "Multivariable Control Allocation and Control Law Conditioning when Control Effectors Limit," *AIAA Guidance, Navigation and Control Conference and Exhibit*, AIAA, Washington, D.C., 1994.

[2] Beck, R. E., "Application of Control Allocation Methods to Linear Systems with Four or More Objectives," Ph.D. Thesis, Virginia Polytechnic Institute and State University, Blacksburg, VA, 2002.

[3] Burken, J. J., Lu, P., Wu, Z., and Bahm, C., "Two Reconfigurable Flight-Control Design Methods: Robust Mechanism and Control Allocation," *Journal of Guidance, Control, and Dynamics*, Vol. 24, No. 3, 2001, pp. 482–493.

[4] Bodson, M., "Evaluation of Optimization Methods for Control Allocation," *Journal of Guidance, Control, and Dynamics*, Vol. 25, No. 4, 2002, pp. 703–711.

[5] Petersen, J. A. M., and Bodson, M., "Interior-Point Algorithms for Control Allocation," *Journal of Guidance, Control, and Dynamics*, Vol. 28, No. 3, May–June 2005, pp. 471–480.

[6] Oh, J.-H., Jamoom, M. B., McConley, M. W., and Feron, E., "Solving Control Allocation Problems Using Semidefinite Programming," *Journal of Guidance, Control, and Dynamics*, Vol. 22, No. 3, May–June 1999, pp. 494–497.

[7] Durham, W. C., "Computationally Efficient Control Allocation," *Journal of Guidance, Control, and Dynamics*, Vol. 24, No. 3, March–April 2001, pp. 369–372.

[8] Boyce, J., and Brosilow, C., "Multivariable Cascade Control for Processes with Output Constraints," *Computer Chemical Engineering*, Vol. 20, No. 2, 1996, pp. 1083–1088.

[9] Lestage, R., Pomerleau, A., and Desbiens, A., "Improved Constrained Cascade Control for Parallel Processes," *Control Engineering Practice*, Vol. 7, No. 8, 1999, pp. 969–974.

[10] Goodwin, G. C., Pérez, T., and De Doná, J. A., *Modeling, Control and Optimization of Complex Systems*, Kluwer Academic Publishers, Norwell, MA, 2002, Chap. 7.

[11] Favier, G., and Da Costa Oliveira, G. H., *Conception de Commandes Robustes*, Hermes Sciences Publications, Paris, 2002, Chap. 9, pp. 317–363.

[12] Bemporad, A., Morari, M., Dua, V., and Pistikopoulos, E. N., "The Explicit Linear Quadratic Regulator for Constrained Systems," *Automatica*, Vol. 38, No. 1, 2002, pp. 3–20.

[13] Findeisen, R., and Allgöwer, F., "An Introduction to Nonlinear Model Predictive Control," *21st Benelux Meeting on Systems and Control*, Technische Universiteit Eindhoven, Eindhoven, The Netherlands, 2002.

[14] McKelvey, T., "Frequency Domain Identification Methods," *Circuits Systems Signal Processing*, Vol. 21, No. 1, 2002, pp. 39–55.

[15] de Vries, D., and Van den Hof, P., "Frequency Domain Identification with Generalized Orthonormal Basis Functions," *IEEE Transactions on Automatic Control*, Vol. 43, No. 5, 1998, pp. 656–669.

[16] Sanathanan, C., and Koerner, J., "Transfer Function Synthesis as a Ratio of Two Complex Polynomials," *IEEE Transactions on Automatic Control*, Vol. AC-8, 1963, pp. 56–58.

[17] Whitfield, A., "Asymptotic Behaviour of Transfer Function Synthesis Methods," *International Journal of Control*, Vol. 45, No. 3, 1987, pp. 1083–1092.

[18] Goldfarb, D., and Idnani, A., "A Numerically Stable Dual Method for Solving Strictly Convex Quadratic Programs," *Mathematical Programming*, Vol. 27, 1983, pp. 1–33.

[19] Schittkowski, K., "QL: A Fortran Code for Convex Quadratic Programming—User's Guide," Department of Mathematics, University of Bayreuth, 2003.

[20] Whitfield, A., "Transfer Function Synthesis Using Frequency Response Data," *International Journal of Control*, Vol. 43, No. 5, 1986, pp. 1413–1426.